

## Impact of punctual flat magnetic shear on the field line transport

C. V. Abud<sup>1</sup> and I. L. Caldas<sup>1</sup>

Citation: *Physics of Plasmas* **22**, 062510 (2015); doi: 10.1063/1.4923016

View online: <http://dx.doi.org/10.1063/1.4923016>

View Table of Contents: <http://aip.scitation.org/toc/php/22/6>

Published by the *American Institute of Physics*

---

---



Small Conferences. BIG Ideas.

Applied Physics  
Reviews

SAVE THE DATE!  
**3D Bioprinting: Physical and Chemical Processes**  
May 2–3, 2017 • Winston Salem, NC, USA

The banner features a background image of a human hand holding a glowing blue, branching structure that resembles a biological or chemical process. The text is overlaid on this image.

# Impact of punctual flat magnetic shear on the field line transport

C. V. Abud<sup>1,2,a)</sup> and I. L. Caldas<sup>2,b)</sup>

<sup>1</sup>Department of Mathematics IMTec, Universidade Federal de Goiás, 75704-020 Catalão, Brazil

<sup>2</sup>Physics Institute, Universidade de São Paulo, 05315-970 São Paulo, Brazil

(Received 26 January 2015; accepted 18 May 2015; published online 24 June 2015)

We investigate the magnetic field line transport for tokamak equilibria with monotonic magnetic shear perturbed by resonant fields. We show that when the local profile is flat at the plasma edge a transport barrier can be created leading to a field line transport reduction. This transport reduction is due to the field lines topological modifications, caused by a local flattened profile that reduces the global field lines escape pattern. The results are obtained by applying a symplectic map that describes perturbed magnetic field lines in large aspect ratio tokamaks. © 2015 AIP Publishing LLC.

[<http://dx.doi.org/10.1063/1.4923016>]

## I. INTRODUCTION

In the last decades, a lot of effort has been dedicated to the improvement of plasma confinement in tokamak devices. A favorable mechanism to improve plasma confinement is the creation of an internal transport barrier (ITB) to reduce the field line escape through the tokamak vessel and, consequently, decrease the local ion thermal diffusivity.<sup>1–3</sup> Among the factors responsible for the existence of ITBs, the shape of the safety factor profile has been shown crucial.<sup>4</sup> One of the ways to investigate ITBs is to consider nonmonotonic safety factor profiles, which gives rise to reversed magnetic shear and the formation of shearless magnetic surfaces. Some experiments using reversed shear related to ITBs can be seen in Ref. 5, where inductive current is used to control the safety factor profile, and in Refs. 6 and 7 for reversed shear generated by neutral beam injection in TFTR and DIII-D tokamaks, respectively. However, evidences support that the formation of ITBs may be also correlated with some local flattening of the otherwise monotonic safety factor.<sup>8,9</sup> In this later case, Hamiltonian models for the magnetic field lines have been shown that a local safety factor profile modification creates a low-shear zone where transport barriers can emerge.

Our main goal with the present paper is to investigate the effects imposed by a safety factor with local flatness, arising either from internal plasma modifications or caused by perturbing external currents, on the transport of magnetic field lines in tokamaks. For that, we perform numerical simulations using a symplectic map introduced to describes chaotic field lines in tokamaks with ergodic limiter.<sup>10</sup> Nonlinear maps have been studied in the context of plasma physics in tokamaks.<sup>10–14</sup> These maps are useful because we do not need to integrate the field line equations over the toroidal revolution; therefore, large scale analysis can be quickly developed. We should note that maps describing the field line transport is a rough approximation of the fast particle transport that neglects the slow drift particles,<sup>15</sup> turbulence fluctuations, and the plasma response.<sup>16</sup> In spite of neglecting these effects, we show that an eventual local flattening in

the magnetic shear profile can locally modify the invariant curves distribution in phase space, modifying significantly the field line transport.

The paper is organized as follows. Section II presents the basic magnetic field line equations, the symplectic map used throughout the paper (Subsection II A), and the introduction of a safety factor with a local flatness point (Subsection II B). We compare the phase spaces obtained by both profiles in Sec. III. Using numerical analysis of the escape pattern and the statistic of the escaping, we discuss in Sec. IV the impact on the transport caused by the safety factor profile with a local flatness point. Section V is devoted to discussions and conclusions.

## II. MAGNETIC FIELD LINES

The toroidal geometry of tokamaks is determined by its major,  $R_0$ , and minor,  $b$ , radii (see scheme in Fig. 1). For large aspect-ratio,  $R_0/b \gg 1$ , we may consider the approximation: periodic cylinder of length  $2\pi R_0$  in coordinates  $(r, \theta, z)$ , whose axis of symmetry,  $z$ , is related with the toroidal angle  $\phi$  by  $z = R_0\phi$ . A point in the tokamak is located by its cylindrical coordinates. However, to study the plasma edge, i.e., the plasma region near the wall, it turns out that even the poloidal curvature does not change the results noticeably, so that a rectangular system can be found by defining the following coordinates:  $x' = b\theta$  and  $y' = b - r$  (Ref. 17) as indicated in Fig. 1(b).

The unperturbed field,  $\mathbf{B}_0$ , is a superposition of two magnetic fields: (i) the toroidal field  $B_\phi = B_z$ , created by external coils and (ii) the poloidal field  $B_\theta$ , due to the plasma current  $I_p$ . In the periodic cylinder approximation, we assume that the toroidal equilibrium field is uniform,  $B_\phi^0 = B_0$ , resulting in the equilibrium magnetic field,  $\mathbf{B}_0(r) = (B_r^0 = 0, B_\theta^0(r), B_0)$ , that represents helical field line curves on a cylindrical surface. Now, consider magnetic perturbations introduced by external magnetic devices of the form  $\mathbf{B}_1(r, \theta, \phi) = (B_r^1(r, \theta, \phi), B_\theta^1(r, \theta, \phi), B_\phi^1 = 0)$ . Thus, the magnetic field lines given by  $\mathbf{B} \times dl = 0$  are

$$\frac{dr}{B_r^1} = \frac{rd\theta}{B_\theta^1} = \frac{R_0d\phi}{B_\phi^0} = \frac{dz}{B_\phi^0}. \quad (1)$$

<sup>a)</sup>cabud@ufg.br

<sup>b)</sup>ibere@if.usp.br

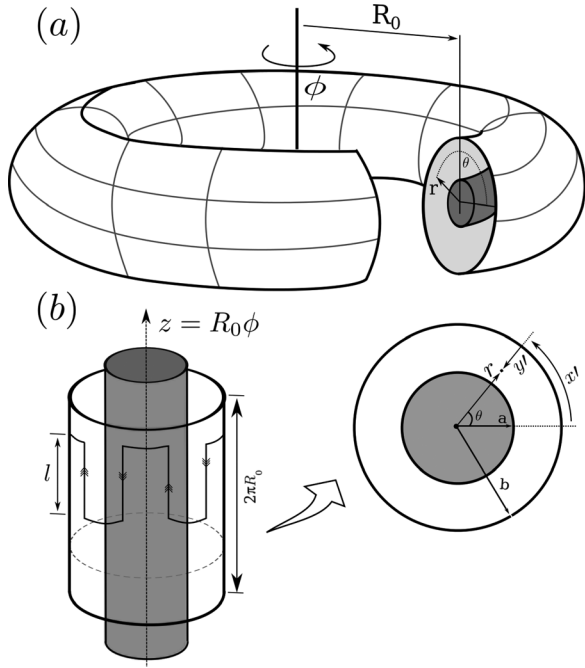


FIG. 1. (a) Tokamak scheme showing the main coordinate systems. (b) The  $2\pi R_0$ -periodic cylindrical approximation where  $l$  is the length of the wires of the EML.

In this paper, we consider perturbations caused by an ergodic magnetic limiter (EML), which consists of a grid-shaped ring of length  $l$  with  $m$  pairs of wires toroidally oriented carrying a current  $I_n$  disposed in the poloidal direction (see Fig. 1). Basically, the main role of the EML is to generate external magnetic fields for destruction of boundary magnetic surfaces.

### A. The symplectic map

We consider a symplectic map that describes the behavior of equilibrium magnetic field lines in the presence of a perturbing magnetic field due to an ergodic limiter. In the absence of perturbation, the magnetic field lines are described by the map<sup>10</sup>

$$F_1 : \begin{cases} r_{n+1} = \frac{r_n}{1 - a_1 \sin \theta} \\ \theta_{n+1} = \theta_n + \frac{2\pi}{q_{eq}(r_{n+1})} + a_1 \cos \theta_n \end{cases}, \quad (2)$$

where  $a_1$  is introduced to take into account a correction for the toroidal geometry. The function  $q_{eq}$  is the equilibrium safety factor that determines the shear of helical magnetic fields, i.e., the mean value of toroidal turns after a complete poloidal turn.

The perturbation map emerges from the effect of the ergodic limiter on the equilibrium configuration. For our purposes, the action of the EML is approximated by a sequence

of delta function pulses at each piercing of a field line in the surface of section. In cylindrical approximation, the map is described by<sup>10</sup>

$$F_2 : \begin{cases} r_{n+1} = r_{n+1}^* + \frac{mC\epsilon b}{m-1} \left(\frac{r_{n+1}^*}{b}\right)^{m-1} \sin(m\theta_{n+1}), \\ \theta_{n+1}^* = \theta_{n+1} - C\epsilon \left(\frac{r_{n+1}^*}{b}\right)^{m-2} \cos(m\theta_{n+1}), \end{cases} \quad (3)$$

where  $C = 2mla^2/R_0q_ab^2$  is the control parameter determined by the experimental set up and  $\epsilon = I_n/I_p$  is the perturbation calculated by the ratio between the perturbing current on the limiter and the equilibrium plasma current. The entire field line mapping is given by the convolution of both maps,  $\hat{F} = F_1 \circ F_2$ . The mapping  $\hat{F}$  is area-preserving, and although this map preserves the magnetic flux only approximately, it is convenient and practical, because we do not have to numerically integrate the field line equations over the toroidal revolution.

### B. Monotonic profile with local flatness

To investigate the effects on the transport caused by local modifications, due either to internal plasma adjustments or external perturbations, we create a local flatness point in the safety factor profile, keeping the profile monotonicity elsewhere. Evidences indicate that the flatness of the rotation profile leads to robustness of the associated invariant curve.<sup>19,20</sup> Indeed, the low shear near to the flatness region is associated with a transport barrier in plasma confined in tokamaks, as experimentally observed in Ref. 9. Here, we intend to modify the monotonic profile proposed in Ref. 18

$$q_{eq}^r(r) = \begin{cases} q_a \frac{r^2}{a^2} \left\{ 1 - \left(1 - \frac{r^2}{a^2}\right)^5 \right\}^{-1} & (0 \leq r \leq a), \\ q_a \frac{r^2}{a^2} & (a \leq r \leq b), \end{cases} \quad (4)$$

where  $q_a$  is the safety factor at the plasma edge  $r = a$ . For numerical simulations, we fixed  $q_a = 5$ .

In Ref. 19, the authors proposed a procedure to create a flattened local position in a monotonic safety factor profile. To introduce a local modification, the safety factor function should depend on three values of  $r$ , namely,  $r_1 < r_0 < r_2$ , where  $r_1$  and  $r_2$  are the local limits and  $r_0$  is the local flatness point. The new smooth function  $q_{eq}^l$  must match  $q_{eq}^r$  on the intervals  $[0; r_1]$  and  $[r_2; 1]$ . And, the derivative in  $r_0$  vanishes, defining the flatness local point. So, a candidate for the safety factor is

$$q_{eq}^l(r) = \begin{cases} q_a \frac{r^2}{a^2} \left\{ 1 - \left(1 - \frac{r^2}{a^2}\right)^5 \right\}^{-1} & (0 \leq r \leq r_1), \\ q_0 - c_1(r - r_0)^7 - c_2(r - r_0)^5 - c_3(r - r_0)^3 & (r_1 \leq r \leq r_2), \\ q_a \frac{r^2}{a^2} & (r_2 \leq r \leq b), \end{cases} \quad (5)$$

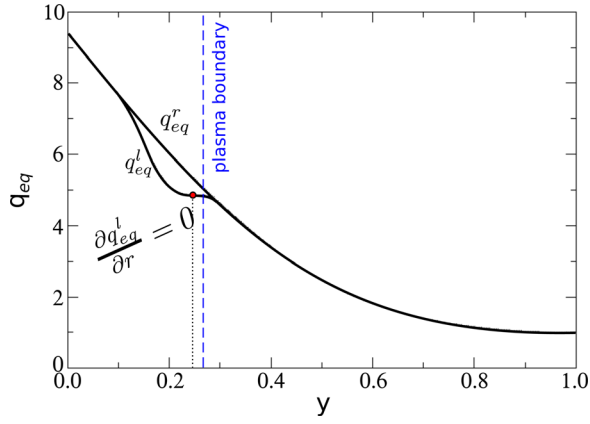


FIG. 2. Monotonic safety factor  $q_{eq}^r$  (Eq. (4)) and the safety factor with a local flatness point  $q_{eq}^l$  (Eq. (5)).

where the coefficients  $q_0$ ,  $c_1$ ,  $c_2$ , and  $c_3$  are obtained using the continuity and derivability of Eq. (5) at the point  $r_1$  and  $r_2$ . In Fig. 2, we show the safety factor profile locally modified in comparison with the monotonic profile  $q_{eq}^r$ . We point out that the flatness point,  $y_0 = 1 - r_0/b$  with  $r_0 = 0.0824$  was placed between the plasma edge and the wall ( $y=0$ ) to induce a transport barrier and alter the plasma-wall interaction. The values  $r_1 = 0.099$  and  $r_2 = 0.077$ , corresponding to  $y=0.1$  and  $y=0.3$  in Fig. 2, are used throughout our simulations.

### III. COMPARING PHASE SPACES

To demonstrate the topological modification caused by the local barrier, we compare the phase spaces for both profiles  $q_{eq}^r$  and  $q_{eq}^l$  using different numbers of coils  $m$  of the ergodic limiter. The amplitude perturbation  $\epsilon$  influences mainly the region situated in the vicinity of the  $m$ -mode

resonant region, i.e., the parameter  $m$ , related to the number of coils of the ergodic limiter, is fundamental with respect to the onset of resonances in the phase space. Figure 3 shows six phase spaces for the symplectic map  $\hat{F}$  with experimental set up given by:  $R_0 = 0.3$  (tokamak major radius),  $a_1 = -0.04$  (toroidal correction),  $a = 0.08$  (plasma radius),  $b = 0.11$  (tokamak minor radius), and  $l = 0.08$  (length of the EML). The first three phase spaces (a)–(c) are obtained with monotonic profile  $q_{eq}^r$  (Eq. (4)) and the last, (d)–(f), using the profile with one flatness point  $q_{eq}^l$  (Eq. (5)). In all cases, we kept the perturbation  $\epsilon = 0.2$ , and the number of coils of the EML for comparison are (a)/(d)  $m=4$ ; (b)/(e)  $m=5$ ; and (c)/(f)  $m=7$ . The first applications, shown in Fig. 3, are obtained for a high value of the perturbation parameter  $\epsilon$  in order to emphasize the robustness of the magnetic topology due to the safety factor flattening. In the chosen examples, the ratio between the external coil current and the plasma current is  $\epsilon = 0.2$ .

In the first case with  $m=4$ , corresponding to phase spaces of Figs. 3(a) and 3(d), we observe that the locally modified profile has changed the region close to the boundary ( $y=0$ ) and the flatness point has induced a regular region composed by invariant curves acting as a barrier to the chaotic layer around the period-four islands. A similar topological changing with respect to the boundary region can be observed in the comparison between Figs. 3(b) and 3(d) for  $m=5$ . Nevertheless, in this case, the perturbation parameter  $\epsilon = 0.2$  is sufficient to destroy any possible barrier caused by the flatness of the safety factor profile. It happens because the mode,  $m=5$ , generates period-five islands where the flatness point is located.

For  $m=7$ , the resonant islands are far enough from the flatness position. Observing Fig. 3(c), we see that the perturbation  $\epsilon = 0.2$  is quite strong for the system guided with  $q_{eq}^r$ .

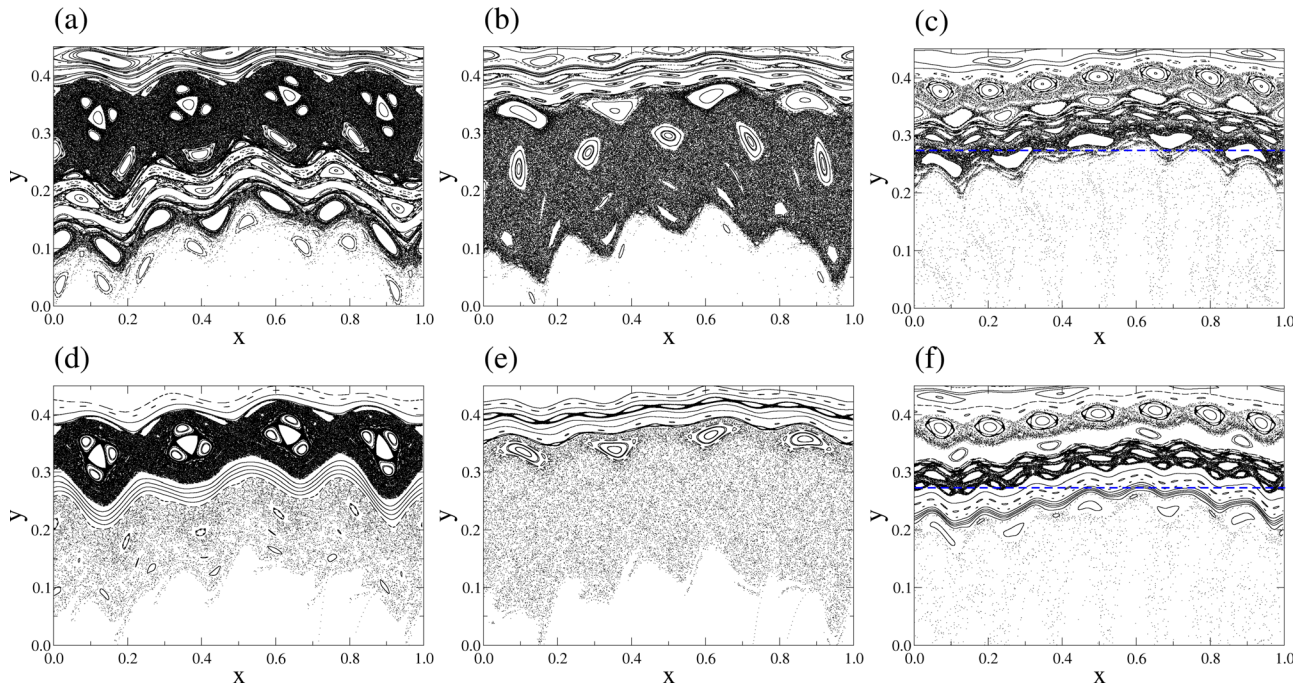


FIG. 3. Phase spaces for the symplectic map  $\hat{F}$  using (a)–(c) monotonic profile,  $q_{eq}^r$ ; (d)–(f) monotonic profile with one flatness point,  $q_{eq}^l$ . For  $\epsilon = 0.2$ , we vary the number of coils  $m$  and the relation to compare the phase spaces are (a)/(d)  $m=4$ ; (b)/(e)  $m=5$ ; (c)/(f)  $m=7$ .

Indeed, all the invariants between the plasma boundary and the wall are destroyed and no effective barrier is present to avoid the escape of trajectories coming from the internal plasma. The introduction of a flatness local point in the safety factor profile changes the phase space, as can be seen in Fig. 3(f). Although the perturbation has destroyed most of the invariants, it was not enough to break the region related to the local flatness point. The remaining invariants curves close to the plasma boundary act as effective transport barriers, isolating the orbits of the region  $y < a$ .

#### IV. IMPACT ON THE TRANSPORT

Our main goal here is to measure the impact caused by local modifications of the safety factor on the transport of orbits. Hence, to quantify such a modification, we compare the transport properties in the phase space guided by  $q_{eq}^l$  and  $q_{eq}^r$ -monotonic profiles. In this case, we set the parameters:  $m = 7$  and  $\epsilon = 0.2$ . Note that by choosing the number of pairs of coils in the ergodic limiter as  $m = 7$ , the perturbation acts mainly on the period-7 resonance, located between the plasma edge and the wall.

To determine the impact of the monotonic profile with local flatness on the transport, we investigate the escape pattern of Figs. 3(c) and 3(f). The region close to the border,  $y = 0$ , is composed by fast escape initial conditions, owing to the perturbation  $\epsilon$  and the number of wires  $m$  of the ergodic limiter. Most of the initial conditions close to the border escape in the first 10 iterations of the map. Therefore, a clear observation of the escape pattern for this region should be associated with fewer iterations. Hence, we have calculated the escape pattern, considering small ranges of 10 iterations, as shown by the color palette of Fig. 4. In this case, the initial conditions that spend more than 100 iterations to hit the tokamak wall have received the same color (dark red).

Figure 4 indicates that the region close to the border of the system is almost entirely filled by initial conditions with fast escape,  $1 < n < 100$ . However, we observe two important modifications: (i) the escape pattern of Fig. 4(a), which refers to the map  $\hat{F}$  with monotonic profile, shows a region close to the plasma boundary  $(x; y) = (0.6; 0.2727)$  that is not observed in Fig. 4(b) due to the existence of the barrier imposed by the local flatness of the safety factor profile; (ii) comparing the amplification of a certain region of Figs. 4(a) and 4(b), we note a significant change in the escape pattern. Indeed, the local flatness has increased the fastest escape regions ( $1 < n < 20$ ) and the thin layer of escapes with  $n > 100$ , on a first examination, cannot be observed anymore in Fig. 4(b).

Finally, to characterize the escape process of the magnetic field lines close to the tokamak wall ( $y = 0$ ), we study the distribution of the escape times of an ensemble of initial conditions. Thus, we computed the escape time statistic (ETS) for a large number of chaotic initial conditions placed within the white square in the left panel of Figs. 4(a) and 4(b). The ETS is defined as

$$\rho(\tau) = \frac{M_n}{M}, \quad (6)$$

where  $M_n$  is the number of initial conditions that crossed the boundary  $y = 0$  with iterations numbers (time)  $n \geq \tau$  and  $M$  is the total number of initial conditions that actually crossed the boundary. In fact, Eq. (6) is a cumulative distribution function that decreases from  $\rho(0) = 1$ . Figure 5 shows the ETS for both cases considering a set of  $10^8$  initial conditions each one iterated  $2 \times 10^6$  times.

As indicated in Fig. 5, the ETS in both cases decays as a power-law with exponents floating in the range  $1 < \gamma < 2$ . For short times,  $\tau < 100$ , both cases present a fast decay and fewer initial conditions remain after 100 iterations of the

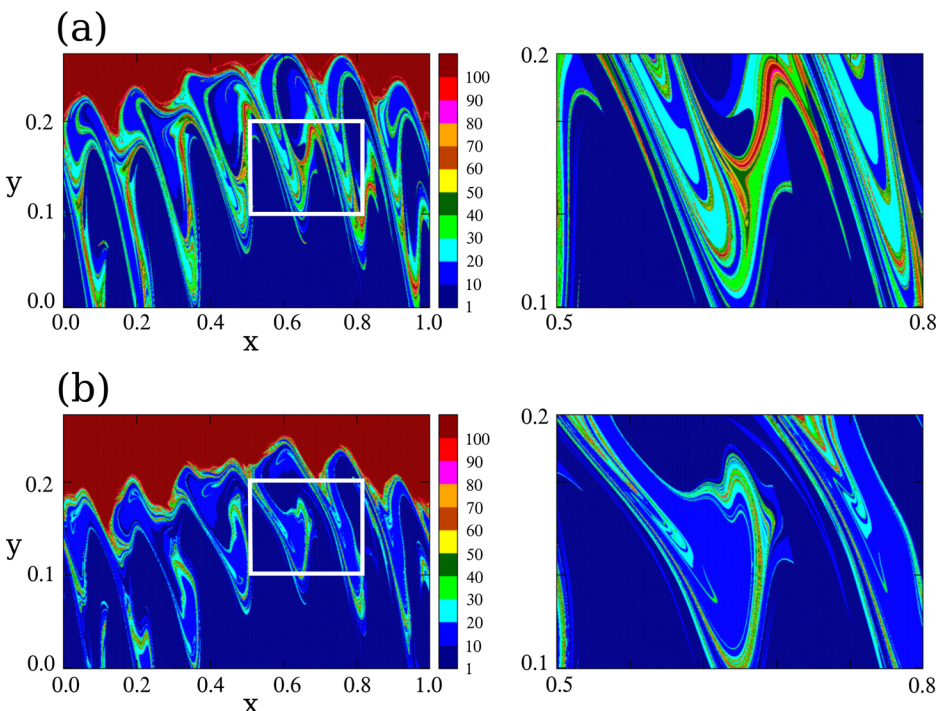


FIG. 4. Escape pattern of the region close to the tokamak border. Phase spaces (a) and (b) can be compared with Figs. 3(c) and 3(f), respectively. The right side of each figure is the amplification of the white square.

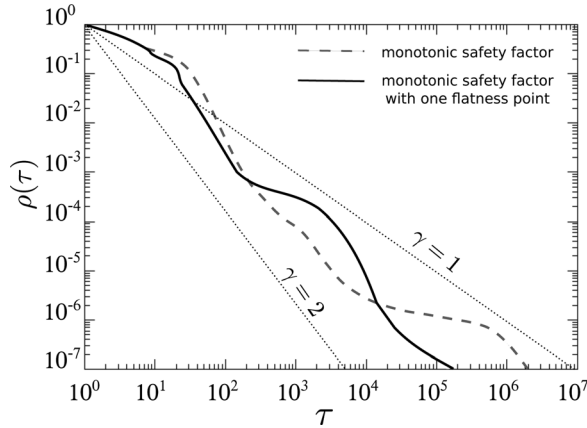


FIG. 5. ETS for a set of initial conditions within the white square in the left panel of Fig. 4(a) monotonic safety factor,  $q_{eq}^r$  (Eq. (4)) and (b) monotonic with a flatness point,  $q_{eq}^l$  (Eq. (5)).

map. Analyzing the range,  $10^3 < \tau < 3 \times 10^3$ , we see that the ETS for the monotonic safety factor with a flatness point (Eq. (5)) decays slower than the monotonic safety factor (Eq. (4)), i.e., the probability of finding initial conditions with time escape belonging to this range is greater for the case with flatness point. Nevertheless, for  $\tau > 10^4$ , the ETS concerning the monotonic safety factor (Eq. (4)) dominates the range of long time escape. It means that the phase space of Fig. 4(b) has a structure that leads some initial conditions to experience up to  $10^6$  iterations without hitting the border  $y=0$ . These long times escape occurs due to the thin layers in the escape pattern of Fig. 4(a) acting as a channel towards the internal region,  $y > a$  (plasma region).

In order to make our approach feasible for experiments in tokamaks, let us consider a smaller perturbation coil current that, e.g., represents 8% of the plasma current,  $\epsilon = 0.08$ . Indeed, the alteration in the safety factor introducing a single flatness point also modifies the topology of the phase space

for weak perturbation as shown in Figs. 6(a) and 6(b). Namely, the area covered by invariant curves around  $y=0.2$  increases. Moreover, the ETS indicates that the set of initial conditions embedded in the chaotic region of the case with safety factor presenting one flatness point tends to escape a little faster than observed in the monotonic case.

## V. CONCLUSIONS

The impact on the transport of magnetic field lines guided by a safety factor with a flatness point (*low shear*) has been analyzed in the context of symplectic maps. Safety factor profiles with local flatness point generates robust barriers in the phase space.<sup>19</sup> We have seen that the plasma-wall interaction is modified by the local flatness point, because it changes the topology of the magnetic surfaces close to the border leading to a fast escape pattern of the trajectories. Comparing phase spaces and analyzing the escape pattern for both: monotonic safety factor (Eq. (4)) and monotonic safety factor with one flatness point (Eq. (5)), we conclude that when the flatness point induces an effective barrier, it may impose two consequences on the dynamics: (i) increase in the confinement, since orbits with  $r < r_0$  do not transpose the barrier and (ii) topological changing of the escape pattern of the magnetic field lines. In this last case, we study the ETS and we identify a specific situation where the onset of the barrier induced a fast escape of the magnetic surfaces, destroying long time channels that lead the trajectories experience long times in the phase space before they hit the border.

From an experimental point of view, particles close to the border that follow the magnetic field lines towards the plasma core and, eventually, escape to the tokamak border are harmful to the plasma confinement.

The power-law decay of the ETS is related to stickiness effects in a certain region or regular structures in the phase

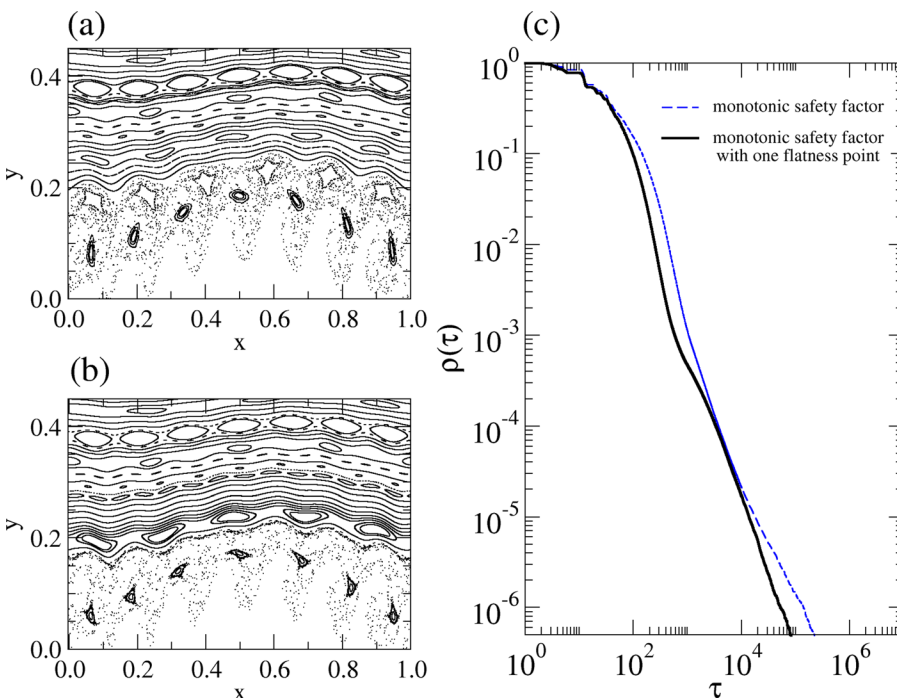


FIG. 6. Phase space of the Ulmann Map with  $\epsilon = 0.08$  and monotonic safety factor,  $q_{eq}^r$  in (a) and monotonic with a flatness point,  $q_{eq}^l$  (Eq. (5)) in (b). In (c), we show the ETS for a set of initial conditions spread in the chaotic region, but not touching the regular islands, for both cases (a) and (b).

space.<sup>21–23</sup> Moreover, the fluctuation of the curves suggests different kinds of dynamical trapping.<sup>24</sup> In our simulation, the stickiness effects are related to the escape channels (see Fig. 4), and the extinction of the long time channels was clearly captured by the ETS.

In principle, the considered local flattening of the safety factor profile could arise as a result of an internal plasma arrangement or be caused by an external perturbation to control the plasma. In such cases, the decrease in transport predicted by this work should be observed for some critical parameters even considering the MHD plasma response, changes in fluctuation, rotation, and a variety of other plasma effects that are not simply understood based on the vacuum field line topology.

## ACKNOWLEDGMENTS

We would like to thank M. C. de Souza for her careful reading of the manuscript, as well as for the fruitful comments and advice that we received from her to improve our manuscript. This work was supported by the Brazilian scientific agencies: CNPq and São Paulo Research Foundation (FAPESP) through Grant Nos. 2013/17989-5 and 2011/19296-1.

- <sup>1</sup>J. W. Connor, T. Fukuda, X. Garbet, C. Gormezano, V. Mukhovatov, M. Wakatani, the ITB Database Group, and the ITPA Topical Group on Transport and Internal Barrier Physics, “A review of internal transport barrier physics for steady-state operation of tokamaks,” *Nucl. Fusion* **44**, R1 (2004).
- <sup>2</sup>C. D. Challis, “The use of internal transport barriers in tokamak plasmas,” *Plasma Phys. Controlled Fusion* **46**, B23 (2004).
- <sup>3</sup>R. C. Wolf, “Internal transport barriers in tokamak plasmas,” *Plasma Phys. Controlled Fusion* **45**, R1 (2003).
- <sup>4</sup>L.-G. Eriksson, C. Fourment, V. Fuchs, X. Litaudon, C. D. Challis, F. Crisanti, B. Esposito, X. Garbet, C. Giroud, N. Hawkes, P. Maget, D. Mazon, and G. Tresset, “Discharges in the JET tokamak where the safety factor profile is identified as the critical factor for triggering internal transport barriers,” *Phys. Rev. Lett.* **88**, 145001 (2002).
- <sup>5</sup>O. Sauter, S. Coda, T. P. Goodman, M. A. Henderson, R. Behn, A. Bottino, E. Fable, An. Martynov, P. Nikkola, C. Zucca, and the TCV team, “Inductive current density perturbations to probe electron internal transport barriers in tokamaks,” *Phys. Rev. Lett.* **94**, 105002 (2005).
- <sup>6</sup>F. M. Levinton, M. C. Zarnstorff, S. H. Batha, M. Bell, R. E. Bell, R. V. Budny, C. Bush, Z. Chang, E. Fredrickson, A. Janos, J. Manickam, A. Ramsey, S. A. Sabbagh, G. L. Schmidt, E. J. Synakowski, and G. Taylor,

- “Improved confinement with reversed magnetic shear in TFTR,” *Phys. Rev. Lett.* **75**, 4417 (1995).
- <sup>7</sup>E. J. Strait, L. L. Lao, M. E. Mauel, B. W. Rice, T. S. Taylor, K. H. Burrell, M. S. Chu, E. A. Lazarus, T. H. Osborne, S. J. Thompson, and A. D. Turnbull, “Enhanced confinement and stability in DIII-D discharges with reversed magnetic shear,” *Phys. Rev. Lett.* **75**, 4421 (1995).
- <sup>8</sup>K. A. Razumova *et al.*, “MHD activity and formation of the electron internal transport barrier in the T-10 tokamak,” *Plasma Phys. Controlled Fusion* **42**, 973 (2000).
- <sup>9</sup>K. A. Razumova *et al.*, “Formation of electron transport barriers under ECR control of the  $q(r)$  profile in the T-10 tokamak,” *Plasma Phys. Rep.* **27**, 273 (2001).
- <sup>10</sup>K. Ullmann and I. L. Caldas, “A symplectic mapping for the ergodic magnetic limiter and its dynamical analysis,” *Chaos, Solitons Fractals* **11**, 2129 (2000).
- <sup>11</sup>S. S. Abdullaev, K. H. Finken, A. Kaleck, and K. H. Spatschek, “Twist mapping for the dynamics of magnetic field lines in a tokamak ergodic divertor,” *Phys. Plasmas* **5**, 196 (1998).
- <sup>12</sup>S. S. Abdullaev, M. Jakubowski, M. Lehnen, O. Schmitz, and B. Unterberg, “On description of magnetic stochasticity in poloidal divertor tokamaks,” *Phys. Plasmas* **15**, 042508 (2008).
- <sup>13</sup>J. S. E. Portela, I. L. Caldas, and R. L. Viana, “Tokamak magnetic field lines described by simple maps,” *Eur. Phys. J. Spec. Top.* **165**, 195 (2008).
- <sup>14</sup>J. D. da Fonseca, D. del-Castillo-Negrete, and I. L. Caldas, “Area-preserving maps models of gyroaverage  $E \times B$  chaotic transport,” *Phys. Plasmas* **21**, 092310 (2014).
- <sup>15</sup>W. Horton, “Drift waves and transport,” *Rev. Mod. Phys.* **71**, 735 (1999).
- <sup>16</sup>H. Frerichs, D. Reiter, O. Schmitz, P. Cahyna, T. E. Evans, Y. Feng, and E. Nardon, “Impact on the screening of resonant magnetic perturbations in three dimensional edge plasma transport simulations for DIII-D,” *Phys. Plasmas* **19**, 052507 (2012).
- <sup>17</sup>T. J. Martin and J. B. Taylor, “Ergodic behavior in a magnetic limiter,” *Plasma Phys. Controlled Fusion* **26**, 321 (1984).
- <sup>18</sup>I. L. Caldas, J. M. Pereira, K. Ullmann, and R. L. Viana, “Magnetic field line mapping for a Tokamak with ergodic limiters,” *Chaos, Solitons Fractals* **7**, 991 (1996).
- <sup>19</sup>D. Constantinescu and M.-C. Firpo, “Modifying locally the safety profile to improve the confinement of magnetic field lines in tokamak plasmas,” *Nucl. Fusion* **52**, 054006 (2012).
- <sup>20</sup>L. Nasi and M.-C. Firpo, “Enhanced confinement with increased extent of the low magnetic shear region in tokamak plasmas,” *Plasma Phys. Controlled Fusion* **51**, 045006 (2009).
- <sup>21</sup>C. V. Abud and I. L. Caldas, “Onset of shearless magnetic surfaces in tokamaks,” *Nucl. Fusion* **54**, 064010 (2014).
- <sup>22</sup>J. D. Meiss, “Symplectic maps, variational principles, and transport,” *Rev. Mod. Phys.* **64**(3), 795 (1992).
- <sup>23</sup>G. M. Zaslavsky, “Chaos, fractional kinetics, and anomalous transport,” *Phys. Rep.* **371**, 461 (2002).
- <sup>24</sup>C. V. Abud and R. E. de Carvalho, “Multifractality, stickiness, and recurrence-time statistics,” *Phys. Rev. E* **88**, 042922 (2013).